

# 1 Differentiation Using Microwave Plasma Torch Desorption Mass 2 Spectrometry of Navel Oranges Cultivated in Neighboring Habitats

3 Xincheng Wang,<sup>†</sup> Meiling Yang,<sup>†</sup> Zhiyuan Wang,<sup>§</sup> Hua Zhang,<sup>†</sup> Guofeng Wang,<sup>†</sup> Min Deng,<sup>‡</sup>  
 4 Huanwen Chen,<sup>\*,†</sup> and Liping Luo<sup>\*,‡,§</sup>

5 <sup>†</sup>Jiangxi Key Laboratory for Mass Spectrometry and Instrumentation, East China University of Technology, Nanchang 330013,  
 6 People's Republic of China

7 <sup>‡</sup>School of Life Sciences, Nanchang University, Nanchang 330031, People's Republic of China

8 <sup>§</sup>Nanchang County the First Secondary School in Liantang, Nanchang 330046, People's Republic of China

9 **S** Supporting Information

10 **ABSTRACT:** The molecular fingerprinting of intact fruit samples combined with statistical data analysis can allow the  
 11 assessment of fruit quality and location of origin. Herein, microwave plasma torch desorption ionization mass spectrometry  
 12 (MPT-MS) was applied to produce molecular fingerprints for the juice sac and exocarp of navel oranges cultivated in three  
 13 closely located habitats, and the mass spectrometric fingerprints were differentiated by principal component analysis (PCA).  
 14 Because of the relatively high temperature and high ionization efficiency of MPT, the volatile aroma compounds and semivolatile  
 15 chemicals in the navel oranges were sensitively detected and confidently identified by collision induced dissociation (CID). The  
 16 limit of detection (LOD) of MPT-MS for vanillin was 0.119  $\mu\text{g/L}$ , with the relative standard deviation (RSD,  $n = 10$ ) of 1.7%.  
 17 The results showed that MPT-MS could be a powerful analytical platform for the sensitive molecular analysis of fruits at  
 18 molecular level with high chemical specificity, allowing differentiation between the same sorts grown in neighboring habitats.

19 **KEYWORDS:** *microwave plasma torch, ambient mass spectrometry, desorption ionization, navel orange, principal component analysis*

## 20 ■ INTRODUCTION

21 Navel orange is a common commodity of citrus containing  
 22 more than 130 beneficial compounds with high nutritional and  
 23 medicinal value to humans.<sup>1</sup> Recent studies have reported that  
 24 sugars are mainly found in juice sac,<sup>1</sup> and ketones, alkenes,  
 25 flavonoids, glycosides, and other volatile flavor compounds are  
 26 mostly contained in the exocarp.<sup>2,3</sup> Although the appearance of  
 27 navel oranges from different habitats is similar, the quality,  
 28 nutrients, and tastes could be significantly different due to the  
 29 difference in cultivation and planting environments, which are  
 30 likely to cause the molecular diversity of the active metabolites  
 31 as well as the nutritional value of navel oranges.

32 Currently, analytical methods such as infrared spectroscopy  
 33 (IR),<sup>4,5</sup> gas chromatography–mass spectrometry (GC–  
 34 MS),<sup>6–8</sup> high performance liquid chromatography  
 35 (HPLC),<sup>9–11</sup> and liquid chromatography–mass spectrometry  
 36 (LC–MS)<sup>12</sup> are typically used for the quality inspection of  
 37 navel oranges. These methods have a high analytical power but  
 38 usually require complicated and time-consuming experimental  
 39 procedures, which hinder high throughput sample analysis.  
 40 Powered by the advent of direct ionization techniques including  
 41 but not limited to desorption electrospray ionization (DESI),<sup>13</sup>  
 42 desorption atmospheric pressure chemical ionization  
 43 (DAPCI),<sup>14,15</sup> extractive electrospray ionization (EESI),<sup>16</sup>  
 44 internal extractive electrospray ionization (iEESI),<sup>17</sup> direct  
 45 analysis in real time (DART),<sup>18</sup> and microwave induced plasma  
 46 (MIP),<sup>19</sup> the speed and simplicity of mass spectrometric  
 47 analysis have dramatically improved. In ambient MS, molecules  
 48 that are easily protonated/deprotonated can be sensitively  
 49 detected by ambient ionization techniques such as DESI, EESI,

and LAESI,<sup>20</sup> which produce analyte ions in a way similar to  
 ESI. It was reported that compounds of weak polarity could be  
 sensitively detected by DAPCI,<sup>21</sup> LTP,<sup>22</sup> and many other  
 ionization methods based on ambient corona discharge.<sup>23</sup>  
 However, the volatile fragrance compounds of navel oranges  
 produce similar MS fingerprints, and different kinds of navel  
 oranges are difficult to distinguish using a sensory method.  
 Therefore, a technique with high desorption and ionization  
 energy would be of interest, because such a technique could  
 provide rich molecular information on the compounds, which  
 are unlikely to be detected by commonly available soft  
 desorption ionization methods.

Microwave plasma torch (MPT),<sup>24</sup> normally used as the  
 excitation source for optical emission spectrophotometry, was  
 employed in analytical mass spectrometry as the ionization  
 source characterized by its relatively high temperature for easy  
 desorption and highly abundant ionic species for effective  
 ionization. So far, MPT-MS has been applied to trace analysis  
 of ambient samples in life sciences, food safety, and public  
 security.<sup>25–27</sup> In this study, MPT-MS was used to directly  
 record the characteristic MS fingerprints of the juice sac and  
 exocarp of navel oranges. The MS data were then subjected to  
 principal component analysis (PCA),<sup>28</sup> which resulted in  
 sensitive differentiation of navel oranges cultivated in three  
 closely located habitats, because MPT-MS provided rich

**Received:** February 5, 2017

**Revised:** March 6, 2017

**Accepted:** March 8, 2017

**Published:** March 8, 2017



75 molecular information on the compounds due to its high  
76 desorption and ionization energy.

## 77 ■ MATERIALS AND METHODS

78 **Reagents and Materials.** The microwave generator (WGY-20,  
79 2450 MHz) and microwave plasma torch tube were provided by  
80 Changchun Jilin Little Swan Instruments Co. Ltd. (Changchun,  
81 China). Chemicals such as methanol (A.R. grade) and standard  
82 substance such as 5-hydroxymethyl furfural, vanillin, and 1-nonanol  
83 were bought from Chinese Chemical Reagent Co. Ltd. (Shanghai,  
84 China). Ultrapurity argon (>99.99%) was purchased from Jiangxi  
85 Guoteng Gas Co. Ltd. (Nanchang, China).

86 Navel oranges (cv. 'Newhall') were collected from three closely  
87 located habitats, which were geologically positioned within 3 km in the  
88 naturally formed farming valleys (Guoxi, Anxi, and Fengxi) at  
89 Yongfeng Town, Xingguo County, Jiangxi Province. The navel orange  
90 trees were 12 years old. The orchard managements were under the  
91 same planting standard for navel oranges. The navel oranges located at  
92 the southern and upper parts of the tree with similar sizes were  
93 harvested on the same day. Prior to analysis, the dust on the orange  
94 surface was washed off by distilled water at room temperature. The  
95 juice sac samples were cut from randomly selected navel oranges, but a  
96 total of 72 exocarp samples were directly sampled by the MPT around  
97 the maximal circle of the navel orange. For better comparison, each  
98 piece of the juice sac (72 samples) was cut into  $10 \times 10 \times 3 \text{ mm}^3$ .

99 **Experimental Method.** All of the experiments were carried out  
100 using a LTQ-XL linear Ion trap mass spectrometer (Finnigan, San  
101 Jose, CA) coupled with a microwave plasma torch (Changchun Jilin  
102 University Little Swan Instruments Co., Ltd., Changchun, China). A  
103 SC102 stepper motor (Beijing Optical Century Instrument Co., Ltd.,  
104 Beijing, China) provided a mobile platform to hold the sample for  
105 analysis.

106 For MS analysis, the MPT device was slightly modified from the  
107 original configuration for atomic emission spectrophotometry  
108 described elsewhere.<sup>29–32</sup> The vertical distance ( $h$ ) between the  
109 sample surface and the plasma torch was 8 mm. The angle ( $\alpha$ )  
110 between the microwave plasma torch and the sample surface was about  
111  $40^\circ$ . The assembly of the MPT was carefully positioned to be coaxial  
112 with the ion entrance capillary of the LTQ mass spectrometer,  
113 allowing a distance ( $d$ ) of 10 mm between the ion entrance and the  
114 MPT (Figure 1). The microwave power was 50 W. The reflected  
115 microwave power was minimized to reach 0 W by adjusting the pipe  
116 pistons of the microwave plasma torch. The flow rate of working gas  
117 (Ar) was 300 mL/min, and the flow rate of the carrier gas (Ar) was  
118 800 mL/min. The positive ion detection mode was used to record the  
119 mass spectra, with the mass range of  $m/z$  50–1000. The LTQ-XL

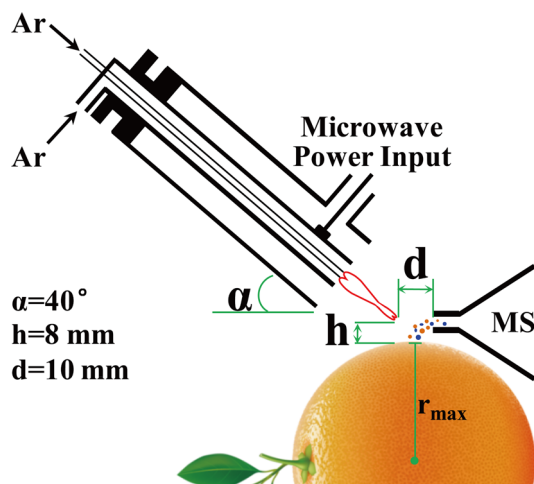


Figure 1. Schematic illustration of microwave plasma torch mass spectrometry for navel orange analysis.

instrument was operated under the following conditions: the capillary  
temperature was  $150^\circ\text{C}$ , the capillary voltage was 16 V, the tube lens  
voltage was 75 V, and the maximum ion injection time was 100 ms.  
For collision induced dissociation (CID) experiments, the mass-to-  
charge ratio window width of 1.2 Da was used to isolate the precursor  
ions. The collision energy was 15–35%, and the collision time was 30  
ms. The rest of the parameters were automatically optimized by tuning  
the LTQ-MS instrument.

## ■ RESULTS AND DISCUSSION

### MPT-MS Analysis of Navel Orange Juice Sac Samples.

The MS fingerprints of juice sac samples were directly recorded  
using MPT-MS under the experimental conditions. Figure 2

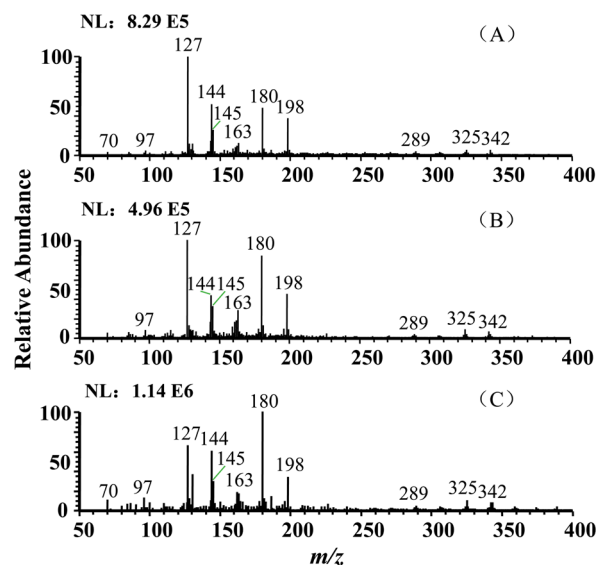
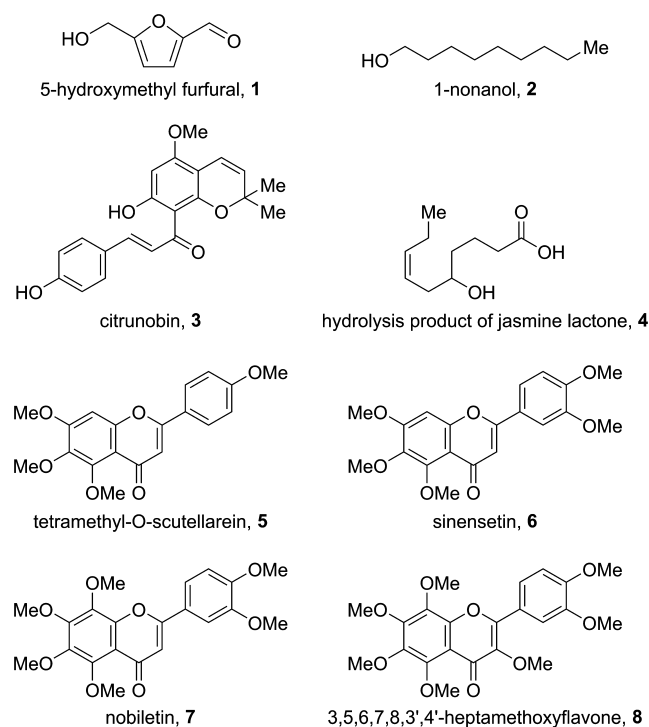
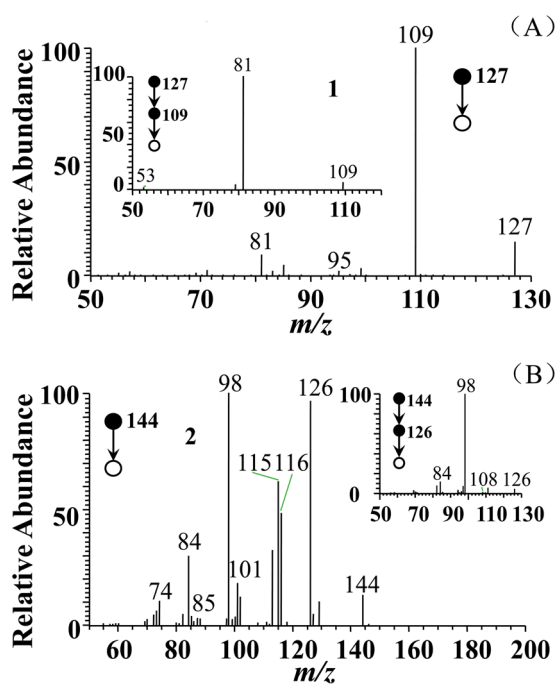


Figure 2. Fingerprint spectra of navel orange juice sac from three origins: (A) Guoxi, (B) Anxi, and (C) Fengxi.

shows the mass spectra of navel orange juice sac samples, with  
dominant peaks at  $m/z$  127, 144, 163, 180, and 198 and small  
peaks such as  $m/z$  289, 325, and 342. Apparently, the  
abundance of these peaks varied along with the juice sac  
samples, showing the correlation between the peaks and the  
habitats. The peak at  $m/z$  127 was tentatively assigned to  
protonated 5-hydroxymethyl furfural (5-HMF), 1 (Figure 3),  
which was favorably produced via degradation of the hexose  
during the heat-assisted desorption ionization process.  
Upon CID, the precursor ion ( $m/z$  127) yielded characteristic  
fragments of  $m/z$  109 and  $m/z$  81 in the MS/MS spectrum  
(Figure 4A), probably by successive loss of  $\text{H}_2\text{O}$  and  $\text{CO}$ . In the  
MS<sup>3</sup> spectrum of  $m/z$  127, the fragment ion at  $m/z$  81 was  
formed by the loss of  $\text{H}_2\text{O}$  and  $\text{CO}$ . The fragmentation pattern  
was in good agreement with that generated using authentic 5-  
HMF, confirming that the  $m/z$  127 peak was due to 5-HMF.  
Note that less 5-HMF is normally found in normal navel  
orange tissue using ESI or low temperature ionization  
techniques (e.g., DAPCI, DESI, EESI); thus the 5-HMF was  
likely formed through the dehydration of hexose caused by  
extensive heating, due to the relatively high temperature of the  
MPT. Therefore, the intensity levels of 5-HMF ( $m/z$  127)  
served as the indicator of hexose, which also fluctuated along  
with the quality/ flavor of navel oranges. In comparison with the  
previous study of metabolites in oranges (*Citrus sinensis*),<sup>1</sup>  
the abundant peak at  $m/z$  180 was assigned to  $[\text{glucosan} + \text{NH}_4]^+$ .  
Similarly, the assignment of peaks at  $m/z$  145 [ $\text{glucosan} -$



**Figure 3.** Chemical structures of 5-hydroxymethyl furfural, **1**, 1-nonanol, **2**, citrunobin, **3**, hydrolysis product of jasmine lactone, **4**, tetramethyl-*O*-scutellarein, **5**, sinensetin, **6**, nobiletin, **7**, and 3,5,6,7,8,3',4'-heptamethoxyflavone, **8**.



**Figure 4.** MS<sup>n</sup> spectra of the main substances of navel orange: (A) 5-HMF (inset: MS<sup>3</sup> spectrum of *m/z* 127); and (B) 1-nonanol (inset: MS<sup>3</sup> spectrum of *m/z* 144).

159 OH]<sup>+</sup>, *m/z* 163 [glucosan+H]<sup>+</sup>, *m/z* 198 [hexose+NH<sub>4</sub>]<sup>+</sup>, *m/z* 160 289 [2glucosan-H<sub>2</sub>O-OH]<sup>+</sup>, *m/z* 325 [2glucosan+H]<sup>+</sup>, and 161 *m/z* 342 [2glucosan+NH<sub>4</sub>]<sup>+</sup> were also enhanced, suggesting 162 that the navel oranges were rich in sugar.<sup>1,37</sup> However, the 163 relative abundance of these peaks varied notably for the navel

orange samples from different habitats. Such differences in 164 sugar levels could partially account for the difference in flavors. 165

Following the strategy for analyte verification, 1-nonanol 166 (MW 144), **2** (Figure 3), a natural product found in navel 167 orange, bitter orange, and many other plant essential oils, was 168 also confidently detected from navel orange juice sacs. Upon 169 CID, the protonated 1-nonanol (*m/z* 144) generated major 170 fragments of *m/z* 126, 116, 115, and 98 (Figure 4B), by the loss 171 of H<sub>2</sub>O, C<sub>2</sub>H<sub>4</sub>, C<sub>2</sub>H<sub>5</sub>, and C<sub>2</sub>H<sub>6</sub>O, respectively. In the MS<sup>3</sup> 172 spectrum of *m/z* 144, the fragment ion at *m/z* 98 was formed 173 by the loss of H<sub>2</sub>O and C<sub>2</sub>H<sub>4</sub>. The CID fragmentation pattern 174 was validated by using authentic 1-nonanol under the same 175 experimental conditions. 176

### MPT-MS Analysis of Navel Orange Exocarp Samples.

MPT-MS was also applied for the direct fingerprinting of navel 178 orange sample pericarp/exocarp, which minimized the potential 179 damages to the fruit, so that the navel oranges could be 180 normally traded as usual. The mass spectrometric fingerprints 181 of exocarp from Guoxi, Anxi, and Fengxi are shown in Figure 182 f5 5A–C, respectively, in which the main peaks at *m/z* 153, 169, 183 f5

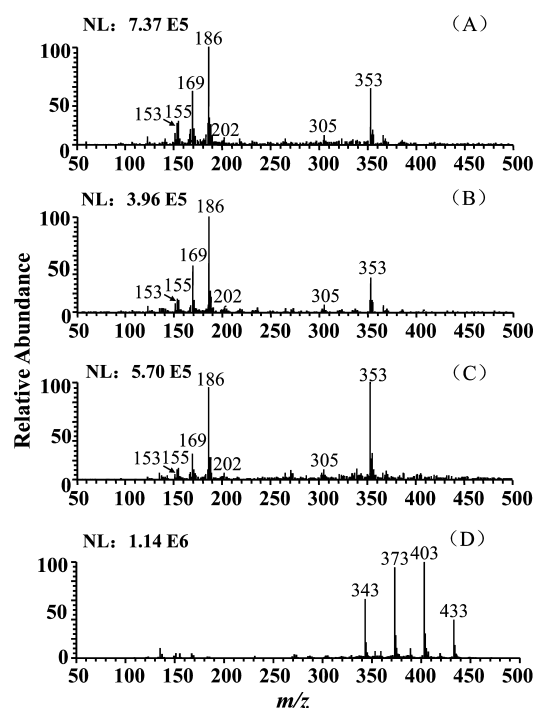


**Figure 5.** Fingerprint spectra of navel orange exocarp from three habitats: (A) Guoxi, (B) Anxi, (C) Fengxi, and (D) Fengxi exocarp heated for more than 30 s.

186, and 353 were detected in every spectrum. However, the 184 relative abundance for these peaks fluctuated considerably, 185 according to the sample habitats. Apparently, the relative 186 abundance of the peak at *m/z* 353 recorded from Fengxi navel 187 oranges (570 000 counts per second (cps)) was significantly 188 higher than those either from Guoxi (265 000 cps) or from 189 Anxi (226 000 cps) navel orange, making the Fengxi oranges 190 outstanding from the other two. Upon CID, the protonated 191 citrunobin, **3** (*m/z* 353), produced major fragments of *m/z* 192 338, 325, and 310, by the loss of (–CH<sub>3</sub>), CO, and (–CH<sub>3</sub> + 193 CO) (Figure 6A), respectively. In comparison with the previous 194 f6 195 study of metabolites in oranges (*Citrus sinensis*), the abundant 195 peak at *m/z* 353 was assigned to be protonated citrunobin,<sup>1,38</sup> 196



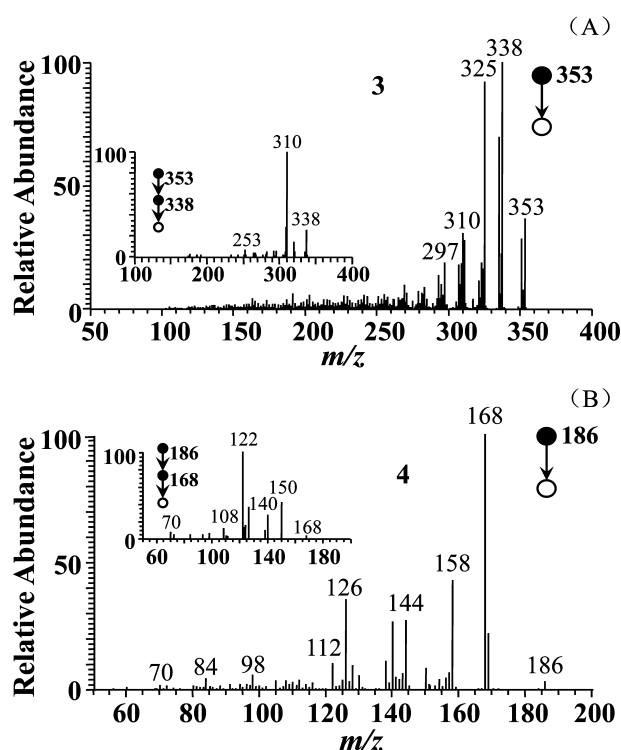


**Figure 6.** MS<sup>2</sup> spectra of the main substance of navel orange: (A) citronobin (inset: MS<sup>3</sup> spectrum of *m/z* 353); and (B) hydrolysis product of jasmine lactone (inset: MS<sup>3</sup> spectrum of *m/z* 186).

197 which is a major type of involatile chalcone (flavonoid) of  
 198 citrus.

199 Similarly, the ion of *m/z* 153 was assigned to protonated  
 200 vanillin. Upon CID, protonated vanillin cleaved H<sub>2</sub>O and CO  
 201 to yield fragments of *m/z* 135 and *m/z* 125, respectively, which  
 202 was consistent with the MS<sup>n</sup> result of vanillin standard obtained  
 203 by MPT-MS. Because vanillin is a major flavor compound in  
 204 orange fruits, it was quantitatively determined by using the  
 205 external standard method.<sup>39</sup> As the result, the relative standard  
 206 deviation (RSD) for vanillin in exocarp was 1.7%, and the limit  
 207 of detection (LOD) was 0.119 μg/L. Quantitative analysis of  
 208 the curve is  $y = 177.7x - 5158$ ,  $R^2 = 0.998$ . The content order  
 209 of vanillin for the navel oranges from these three habitats is  
 210 Guoxi > Fengxi > Anxi.

211 Jasmine lactone (MW 168) is a natural compound providing  
 212 sweet, flowery, and fruity flavors. In our case, the peaks at *m/z*  
 213 169 and 186 were detected in the full-scan mass spectra of  
 214 exocarp samples (Figure 5A–C). Subjection of *m/z* 169 to CID  
 215 resulted in the formation of *m/z* 151, 141, 127, 109, and 95 by  
 216 the loss of (H<sub>2</sub>O), (CO), (COCH<sub>2</sub>-), (-CH<sub>3</sub>COOH), and  
 217 (-CH<sub>3</sub>CH<sub>2</sub>COOH), respectively, which had the fragmentation  
 218 pattern similar to that in the GC-MS analysis of jasmine

lactone.<sup>40</sup> According to previous reports,<sup>41,42</sup> the peaks at *m/z* 219  
 169 and 186 were the signs of jasmine lactone when analyzing 220  
 gardenia and fruits of citrus. Thus, the detection of the peak at 221  
*m/z* 186 (Figure 5A–C) also indicated the existence of jasmine 222  
 lactone in navel orange exocarp samples. Therefore, the peak at 223  
*m/z* 169 was tentatively identified as protonated jasmine 224  
 lactone. The peak at *m/z* 186 was probably the protonated 225  
 product of jasmine lactone after hydrolysis, 4 (Figure 3). 226  
 During the CID process, the precursor ion (*m/z* 186) 227  
 generated peaks at *m/z* 168, 158, 144, 126, and 112 by the 228  
 loss of (H<sub>2</sub>O), (CO), (COCH<sub>2</sub>-), (-CH<sub>3</sub>COOH), and 229  
 (-CH<sub>3</sub>CH<sub>2</sub>COOH) (Figure 6B), respectively. Note that the 230  
 ion of *m/z* 186 and the MS<sup>2</sup> ion of *m/z* 168 (Figure 6B, inset) 231  
 may have a fragmentation pattern similar to that of protonated 232  
 jasmine lactone (*m/z* 169), although the hydrolysis might affect 233  
 the fragmentation pattern of the lactone. The small peak at *m/z* 234  
 155 was ascribed to protonated nerol or geraniol, which is 235  
 widespread in Rutaceae.<sup>43,44</sup> 236

More interestingly, a group of peaks at *m/z* 343, 373, 403, 237  
 and 433 corresponding to polymethoxyflavones (PMFs) 238  
 appeared in the spectrum (Figure 5D) when the navel orange 239  
 exocarp was heated by MPT for more than 30 s. The detection 240  
 of PMFs was confirmed by comparing the multiple-stage 241  
 tandem mass spectra (Table 1) with the MS<sup>n</sup> results in previous 242  
 studies.<sup>45,46</sup> It was worth noting that few peaks were detected in 243  
 the low mass range accompanying the PMFs, because the small 244  
 analytes with a low mass-to-charge ratio were of high volatility 245  
 and were almost evaporated before the PMFs were desorbed by 246  
 MPT. For reference, only a few peaks rather than the PMFs at 247  
 lower mass range were detected by DAPCI-MS,<sup>47</sup> indicating 248  
 that the heating process facilitated by MPT was necessary for 249  
 PMFs detection. More specifically, the peaks at *m/z* 343, 373, 250  
 403, and 433 corresponded to tetramethyl-*o*-scutellarein, 5, 251  
 sinensetin, 6, nobiletin, 7, and 3,5,6,7,8,3',4'-heptamethoxy- 252  
 flavone, 8 (Figure 3), respectively.<sup>47</sup> In the CID spectrum, their 253  
 fragmentation patterns are consistent with each other by the 254  
 loss of 15, 30, and 61 Da, corresponding to (CH<sub>3</sub>-), 255  
 (CH<sub>2</sub>O-), and (2CH<sub>3</sub>O - H), respectively.<sup>47</sup> Table 1 256  
 summarizes the CID data and signal intensity levels of the 257  
 PMFs. As shown in Table 1, the signal intensity levels of *m/z* 258  
 343, 403, and 433, which corresponded to 991 000, 2 030 000, 259  
 and 758 000 cps, respectively, in Fengxi navel oranges were the 260  
 highest among the three types of navel oranges. For sinensetin 261  
 (*m/z* 373), the signal intensity level in Fengxi navel oranges 262  
 was only slightly lower than that in Anxi. In general, the content 263  
 of PMFs was rich in Fengxi navel oranges. As the bioactive 264  
 plant components in the orange peels, PMFs can be used to 265  
 inhibit the growth of a variety of cancer cells, mutant cells, and 266  
 to reduce the oxygen stress of cells. Presumably, the higher 267  
 content of PMFs in fruits would bring more benefit to 268  
 consumers. Therefore, as indicated in Table 1, the level of 269  
 nobiletin was found to be highest in Fengxi navel oranges. The 270

**Table 1.** Polymethoxyflavones Fragments and Signal Intensity Levels of Navel Orange Exocarp Samples

structure number	name	<i>m/z</i>	main fragments	intensity		
				Guoxi	Anxi	Fengxi
5	tetramethyl- <i>O</i> -scutellarein	343	328, 313, 299, 282	964000	935000	991000
6	sinensetin	373	358, 343, 329, 312	1500000	1840000	1830000
7	nobiletin	403	388, 373, 355, 342, 327	1500000	1860000	2030000
8	3,5,6,7,8,3',4'-heptamethoxyflavone	433	418, 403, 385, 372, 342	528000	696000	758000
total/intensity				4490000	5330000	5600000

271 detection of PMFs demonstrated that, assisted by heating,  
 272 MPT favored desorption/ionization of typical nonvolatile  
 273 compounds embedded even deeply in plant tissue, which  
 274 might not be detectable using other ionization techniques such  
 275 as DAPCI or DESI due to the lack of heating for efficient  
 276 desorption.

277 **Visualization of the Differences among Navel**  
 278 **Oranges.** The MS fingerprints of navel orange juice sacs  
 279 (Figure 2) and exocarp (Figure 5) showed notable differences  
 280 for the navel oranges cultivated in the three habitats. To easily  
 281 visualize the recognition, a multivariate statistic tool, principal  
 282 component analysis (PCA), was employed to process the MS  
 283 fingerprints data.<sup>48</sup> For example, Figure 7A shows the PCA

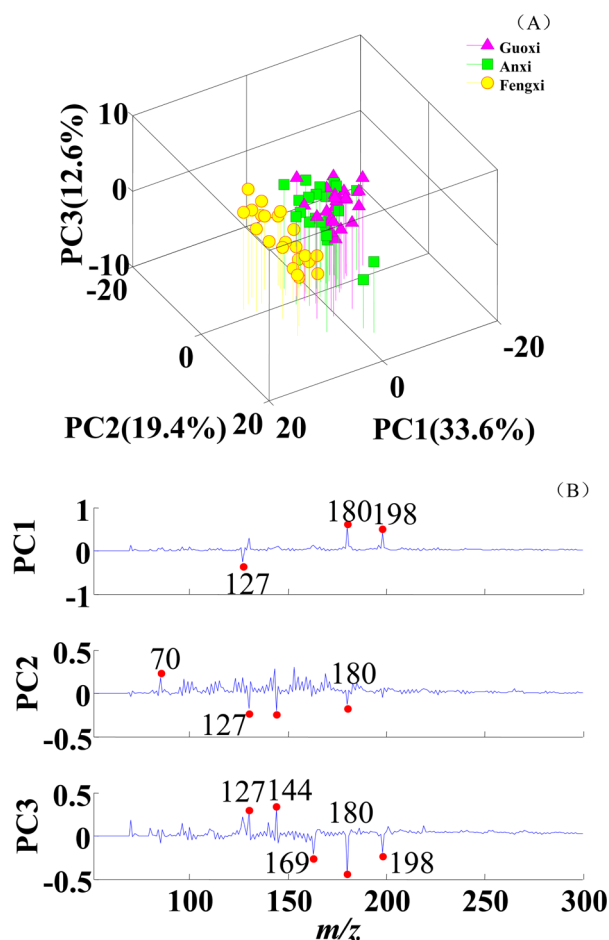


Figure 7. PCA score results of navel orange juice sac composition: (A) 3D-PCA score plot; and (B) PCA loading plots.

284 score plots obtained using MPT-MS with 72 individual juice sac  
 285 samples, in which the samples collected from Fengxi were  
 286 separated from those cultivated in either Guoxi or Anxi habitat.  
 287 The Anxi navel oranges were almost as uniformly distributed in  
 288 the 3-D PCA score plots as the Guoxi samples, showing that no  
 289 significant difference was detected by MPT-MS from the juice  
 290 sac samples, although the samples were cultivated in two  
 291 habitats located in vicinity. The loading plots shown in Figure  
 292 7B indicated that sugars were the major differential ingredients  
 293 among the navel oranges tested.

294 Similar to Figure 7A, the 72 navel oranges from Fengxi were  
 295 clearly separated from the rest of the samples (Figure 8A) when  
 296 PCA was applied to processing the MPT-MS fingerprints of

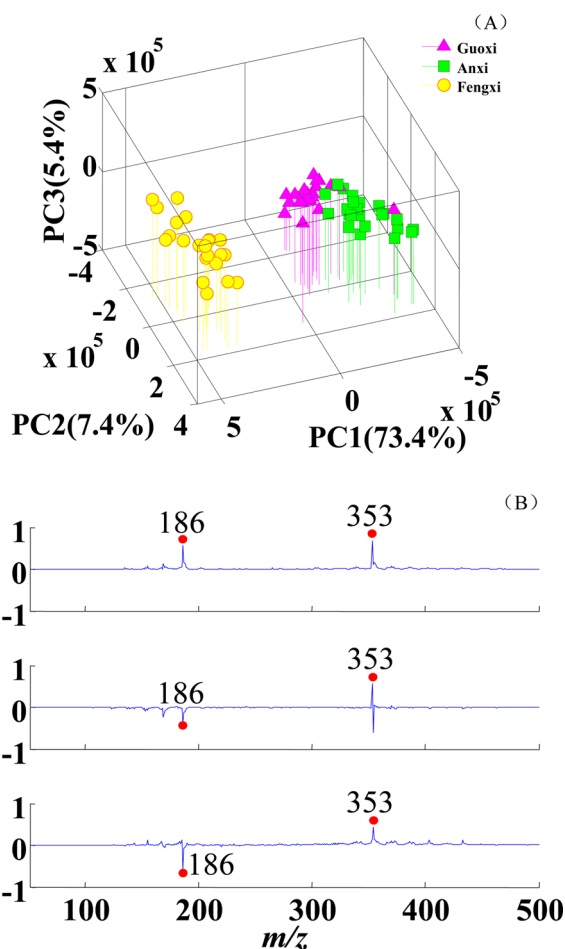


Figure 8. PCA score results of navel orange exocarp composition: (A) 3D-PCA score plot; and (B) PCA loading plots.

navel orange exocarp samples. However, both the Guoxi 297  
 samples and the Anxi samples were tightly clustered in Figure 298  
 8A, resulting in better separation of the three types of navel 299  
 orange samples. The improved differentiation was achieved by 300  
 the differential analytes, that is, the major signals of citronobin 301  
 ( $m/z$  353) and hydrolysis product of jasmine lactone ( $m/z$  302  
 186) in the loading plots (Figure 8B), which were quite 303  
 different from those shown in Figure 7B. Overall, the exocarp 304  
 samples were better than the juice sacs samples for MPT-MS 305  
 differential analysis of navel oranges cultivated in closely located 306  
 habitats, providing easy access, fast analysis speed, and 307  
 satisfactory differentiation. 308

In conclusion, the volatile aroma compounds such as vanillin, 309  
 and semivolatiles chemicals such as sugars, alcohols, and 310  
 anticancer flavonoids in the juice sacs and exocarps of navel 311  
 oranges, were sensitively detected by microwave plasma torch 312  
 desorption ionization mass spectrometry (MPT-MS) followed 313  
 by the statistical data analysis. Fast recognition of the quality 314  
 and origin of fruits produced in three closely located habitats 315  
 (Guoxi, Anxi, and Fengxi) was successfully achieved. The 316  
 differentiation quality was notably improved by using MPT-MS 317  
 data recorded from navel orange exocarp samples rather than 318  
 the juice sac samples. The data thus demonstrate that MPT-MS 319  
 is a sensitive analytical technique to reveal the differential 320  
 information at the molecular level without invasive sample 321  
 manipulation and is a promising method to allow distinction 322  
 between the same types grown in neighboring vicinities. 323

## 324 ■ ASSOCIATED CONTENT

## 325 ● Supporting Information

326 The Supporting Information is available free of charge on the  
327 ACS Publications website at DOI: 10.1021/acs.jafc.7b00553.

328 Tandem mass spectra of vanillin and jasmine lactone in  
329 the navel oranges by MPT-MS; tandem mass spectra of  
330 5-HMF standard, 1-nonanol standard, and vanillin  
331 standard obtained by MPT-MS; tandem mass spectra  
332 of the PMFs in the navel oranges by MPT-MS; and the  
333 RSD, LOD, and quantitative analysis curve of vanillin  
334 (PDF)

## 335 ■ AUTHOR INFORMATION

## 336 Corresponding Authors

337 \*E-mail: ????

338 \*Tel.: +86-0791-83969519. Fax: +86-0791-83969519. E-mail:

339 lluo2@126.com.

340 ORCID 

341 Liping Luo: 0000-0002-6510-8421

## 342 Funding

343 This work was supported by the National Key Scientific  
344 Instrument Development Projects (2011YQ14015008), the  
345 Program for Changjiang Scholars and Innovative Research  
346 Team in University (PCSIRT) (no. IRT13054), and Interna-  
347 tional Science & Technology Cooperation Program (no.  
348 2015DFA40290).

## 349 Notes

350 The authors declare no competing financial interest.

## 351 ■ REFERENCES

- 352 (1) Pan, Z. Y.; Li, Y.; Deng, X. X.; Xiao, S. Y. Non-targeted  
353 metabolomic analysis of orange (*Citrus sinensis* L. Osbeck) wild type  
354 and bud mutant fruits by direct analysis in real-time and HPLC-  
355 electrospray mass spectrometry. *Metabolomics* **2014**, *10*, 508–523.
- 356 (2) Anagnostopoulou, M. A.; Kefalas, P.; Kokkalou, E.;  
357 Assimopoulou, A. N.; Papageorgiou, V. P. Analysis of antioxidant  
358 compounds in sweet orange peel by HPLC–diode array detection–  
359 electrospray ionization mass spectrometry. *Biomed. Chromatogr.* **2005**,  
360 *19*, 138–148.
- 361 (3) Dharmawan, J.; Barlow, P. J.; Curran, P. Characterisation of  
362 volatile compounds in selected citrus fruits from Asia. *Dev. Food Sci.*  
363 **2006**, *43*, 319–322.
- 364 (4) Liu, Y. D.; Zhou, Y. R.; Pan, Y. Y. Online quantitative analysis of  
365 soluble solids content in navel oranges using visible-near infrared  
366 spectroscopy and variable selection methods. *J. Innovative Opt. Health*  
367 *Sci.* **2014**, *7*, 1350065.
- 368 (5) Kelebek, H.; Selli, S. Determination of volatile, phenolic, organic  
369 acid and sugar components in a Turkish cv. Dortyol (*Citrus sinensis* L.  
370 Osbeck) orange juice. *J. Sci. Food Agric.* **2011**, *91*, 1855–1862.
- 371 (6) Cerdán-Calero, M.; Izquierdo, L.; Halket, J. M.; Sentandreu, E.  
372 Evaluation of minimal processing of orange juice by automated data  
373 analysis of volatiles and nonvolatile polar compounds determined by  
374 gas chromatography coupled to mass spectrometry. *Int. J. Food Sci.*  
375 *Technol.* **2014**, *49*, 1432–1440.
- 376 (7) Gómez-Ariza, J. L.; García-Barrera, T.; Lorenzo, F. Determination  
377 of flavour and off-flavour compounds in orange juice by on-line  
378 coupling of a pervaporation unit to gas chromatography–mass  
379 spectrometry. *J. Chromatogr. A* **2004**, *1047*, 313–317.
- 380 (8) McCalley, D. V.; Torres-Grifol, J. F. Analysis of volatiles from  
381 oranges in good and bad condition by gas chromatography and gas  
382 chromatography-mass spectrometry. *Analyst* **1992**, *117*, 721–725.
- 383 (9) Gómez-Ariza, J. L.; Villegas-Portero, M. J.; Bernal-Daza, V.  
384 Characterization and analysis of amino acids in orange juice by

HPLC–MS/MS for authenticity assessment. *Anal. Chim. Acta* **2005**, *385*  
*540*, 221–230. 386

(10) Scherer, R.; Rybka, A. C. P.; Ballus, C. A.; Meinhart, A. D.;  
387 Teixeira Filho, J.; Godoy, H. T. Validation of a HPLC method for  
388 simultaneous determination of main organic acids in fruits and juices. 389  
*Food Chem.* **2012**, *135*, 150–154. 390

(11) Camarda, L.; Di Stefano, V.; Del Bosco, S. F.; Schillaci, D.  
391 Antiproliferative activity of citrus juices and HPLC evaluation of their  
392 flavonoid composition. *Fitoterapia* **2007**, *78*, 426–429. 393

(12) Hu, L.; Lei, S. R.; Guo, L. A. Determination of citrus red 2 in  
394 navel orange by ultra performance liquid chromatography-tandem  
395 mass spectrometry. *Sepeu* **2012**, *30*, 832–835. 396

(13) Takáts, Z.; Wiseman, J. M.; Gologan, B.; Cooks, R. G. Mass  
397 spectrometry sampling under ambient conditions with desorption  
398 electrospray ionization. *Science* **2004**, *306*, 471–473. 399

(14) Chen, H. W.; Liang, H. Z.; Ding, J. H.; Lai, J. H.; Huan, Y. F.;  
400 Qiao, X. L. Rapid differentiation of tea products by surface desorption  
401 atmospheric pressure chemical ionization mass spectrometry. *J. Agric.*  
*Food Chem.* **2007**, *55*, 10093–10100. 403

(15) Wu, Z. C.; Chen, H. W.; Wang, W. L.; Jia, B.; Yang, T. L.; Zhao,  
404 Z. F.; Ding, J. H.; Xiao, X. X. Differentiation of dried sea cucumber  
405 products from different geographical areas by surface desorption  
406 atmospheric pressure chemical ionization mass spectrometry. *J. Agric.*  
*Food Chem.* **2009**, *57*, 9356–9364. 408

(16) Chen, H. W.; Yang, S. P.; Li, M.; Hu, B.; Li, J. Q.; Wang, J.  
409 Sensitive detection of native proteins using extractive electrospray  
410 ionization mass spectrometry. *Angew. Chem., Int. Ed.* **2010**, *49*, 3053–  
411 3056. 412

(17) Zhang, H.; Gu, H. W.; Yan, F. Y.; Wang, N. N.; Wei, Y. P.; Xu, J.  
413 J.; Chen, H. W. Direct characterization of bulk samples by internal  
414 extractive electrospray ionization mass spectrometry. *Sci. Rep.* **2013**, *3*,  
415 2495. 416

(18) Cody, R. B.; Laramée, J. A.; Durst, H. D. Versatile new ion  
417 source for the analysis of materials in open air under ambient  
418 conditions. *Anal. Chem.* **2005**, *77*, 2297–2302. 419

(19) Zhan, X. F.; Zhao, Z. J.; Yuan, X.; Wang, Q. H.; Li, D. D.; Xie,  
420 H.; Li, X. M.; Zhou, M. G.; Duan, Y. X. Microwave-induced plasma  
421 desorption/ionization source for ambient mass spectrometry. *Anal.*  
*Chem.* **2013**, *85*, 4512–4519. 423

(20) Shrestha, B.; Nemes, P.; Nazarian, J.; Hathout, Y.; Hoffman, E.  
424 P.; Vertes, A. Direct analysis of lipids and small metabolites in mouse  
425 brain tissue by AP IR-MALDI and reactive LAESI mass spectrometry.  
426 *Analyst* **2010**, *135*, 751–758. 427

(21) Huang, X. Y.; Guo, X. L.; Luo, H. L.; Fang, X. W.; Zhu, T. G.;  
428 Zhang, X. L.; Chen, H. W.; Luo, L. P. Fast differential analysis of  
429 propolis using surface desorption atmospheric pressure chemical  
430 ionization mass spectrometry. *Int. J. Anal. Chem.* **2015**, *2015*, 176475. 431

(22) Garcia-reyes, J. F.; Harper, J. D.; Salazar, G. A.; Charipar, N. A.;  
432 Ouyang, Z.; Cooks, R. G. Detection of explosives and related  
433 compounds by low-temperature plasma ambient ionization mass  
434 spectrometry. *Anal. Chem.* **2010**, *83*, 1084–1092. 435

(23) Yu, Z.; Chen, L. C.; Suzuki, H.; Ariyada, O.; Erra-Balsells, R.;  
436 Nonami, H.; Hiraoka, K. Direct profiling of phytochemicals in tulip  
437 tissues and in vivo monitoring of the change of carbohydrate content  
438 in tulip bulbs by probe electrospray ionization mass spectrometry. *J.*  
*Am. Soc. Mass Spectrom.* **2009**, *20*, 2304–2311. 440

(24) Jin, Q. H.; Zhu, C.; Borer, M. W.; Hieftje, G. M. A microwave  
441 plasma torch assembly for atomic emission spectrometry. *Spectrochim.*  
*Acta, Part B* **1991**, *46*, 417–430. 443

(25) Wan, T. Q.; Yu, D. D.; Zhang, T. Q.; Zhang, X. W.; Zhou, J. G.  
444 A rapid method for detection of gunshot residue using microwave  
445 plasma torch-mass spectrometry. *Procedia Eng.* **2010**, *7*, 22–27. 446

(26) Zhang, T. Q.; Zhou, W.; Jin, W.; Zhou, J. G.; Handberg, E.; Zhu,  
447 Z. Q.; Huan, W. C.; Jin, Q. H. Direct desorption/ionization of analytes  
448 by microwave plasma torch for ambient mass spectrometric analysis. *J.*  
*Mass Spectrom.* **2013**, *48*, 669–676. 450

(27) Li, Y.; Yang, M. L.; Sun, R.; Zhong, T.; Chen, H. W. Detection  
451 of uranium in industrial and mines samples by microwave plasma torch  
452 mass spectrometry. *J. Mass Spectrom.* **2016**, *51*, 159–164. 453



- 454 (28) Zhu, L.; Yan, J. P.; Zhu, Z. Q.; Ouyang, Y. Z.; Zhang, X. L.;  
455 Zhang, W. J.; Dai, X. M.; Luo, L. P.; Chen, H. W. Differential analysis  
456 of camphor wood products by desorption atmospheric pressure  
457 chemical ionization mass spectrometry. *J. Agric. Food Chem.* **2013**, *61*,  
458 547–552.
- 459 (29) Duan, Y. X.; Du, X. G.; Jin, Q. H. Comparative studies of  
460 surfatron and microwave plasma torch sources for determination of  
461 mercury by atomic emission spectrometry. *J. Anal. At. Spectrom.* **1994**,  
462 *9*, 629–633.
- 463 (30) Yang, W. J.; Zhang, H. Q.; Yu, A. M.; Jin, Q. H. Microwave  
464 plasma torch analytical atomic spectrometry. *Microchem. J.* **2000**, *66*,  
465 147–170.
- 466 (31) Liang, F.; Zhang, D. I.; Lei, Y. H.; Zhang, H. Q.; Jin, Q. H.  
467 Determination of selected noble metals by MPT-AES using a  
468 pneumatic nebulizer. *Microchem. J.* **1995**, *52*, 181–187.
- 469 (32) Gong, Z.; Chan, W. F.; Wang, X.; Lee, F. S.-C. Determination of  
470 arsenic and antimony by microwave plasma atomic emission  
471 spectrometry coupled with hydride generation and a PTFE membrane  
472 separator. *Anal. Chim. Acta* **2001**, *450*, 207–214.
- 473 (33) Rajchl, A.; Drgová, L.; Grégrová, A.; Čížková, H.; Ševčík, R.;  
474 Voldřich, M. Rapid determination of 5-hydroxymethylfurfural by  
475 DART ionization with time-of-flight mass spectrometry. *Anal. Bioanal.*  
476 *Chem.* **2013**, *405*, 4737–4745.
- 477 (34) Zakrzewska, M. E.; Bogel-Łukasik, E.; Bogel-Łukasik, R. Ionic  
478 liquid-mediated formation of 5-hydroxymethylfurfural-A promising  
479 biomass-derived building block. *Chem. Rev.* **2010**, *111*, 397–417.
- 480 (35) Román-Leshkov, Y.; Chheda, J. N.; Dumesic, J. A. Phase  
481 modifiers promote efficient production of hydroxymethylfurfural from  
482 fructose. *Science* **2006**, *312*, 1933–1937.
- 483 (36) Chheda, J. N.; Román-Leshkov, Y.; Dumesic, J. A. Production of  
484 5-hydroxymethylfurfural and furfural by dehydration of biomass-  
485 derived mono- and poly-saccharides. *Green Chem.* **2007**, *9*, 342–350.
- 486 (37) Chernetsova, E. S.; Morlock, G. E. Assessing the capabilities of  
487 direct analysis in real time mass spectrometry for 5-hydroxymethyl-  
488 furfural quantitation in honey. *Int. J. Mass Spectrom.* **2012**, *314*, 22–32.
- 489 (38) Wu, T. S. Flavonoids from root bark of *Citrus sinensis* and  
490 *C. nobilis*. *Phytochemistry* **1989**, *28*, 3558–3560.
- 491 (39) Averbeck, M.; Schieberle, P. H. Characterisation of the key  
492 aroma compounds in a freshly reconstituted orange juice from  
493 concentrate. *Eur. Food Res. Technol.* **2009**, *229*, 611–622.
- 494 (40) Casilli, A.; Decorzant, E.; Jaquier, A.; Delort, E. Multidimen-  
495 sional gas chromatography hyphenated to mass spectrometry and  
496 olfactometry for the volatile analysis of citrus hybrid peel extract. *J.*  
497 *Chromatogr. A* **2014**, *1373*, 169–178.
- 498 (41) Liang, H. Z.; Zhang, X.; Chen, S. X.; Shao, Z. Corona discharge  
499 atmospheric pressure ionization mass spectrometry for real time gas  
500 analysis. *Chin. J. Anal. Chem.* **2008**, *36*, 1152–1156.
- 501 (42) Delort, E.; Casilli, A.; Decorzant, E.; Jaquier, A. Identification of  
502 new volatile compounds in the Citrus Hybrid Mandarinquat 'Indio'.  
503 *Acta Hort.* **2015**, *1065*, 293–303.
- 504 (43) Hamdan, D. I.; Mohamed, M. E.; Abdulla, R. H.; Mohamed, S.  
505 M.; El-Shazly, A. M. Anti-inflammatory, insecticidal and antimicrobial  
506 activities and chemical composition of the essential oils of different  
507 plant organs from navel orange (*Citrus sinensis* L.) Osbeck var. Malesy)  
508 grown in Egypt. *J. Med. Plants Res.* **2013**, *7*, 1204–1215.
- 509 (44) Kelebek, H.; Selli, S. Determination of volatile, phenolic, organic  
510 acid and sugar components in a Turkish cv. Dortyol (*Citrus sinensis* L.  
511 Osbeck) orange juice. *J. Sci. Food Agric.* **2011**, *91*, 1855–1862.
- 512 (45) Winkel-Shirley, B. It takes a garden. how work on diverse plant  
513 species has contributed to an understanding of flavonoid metabolism.  
514 *Plant Physiol.* **2001**, *127*, 1399–1404.
- 515 (46) Ye, X. L.; Cao, D.; Zhao, X.; Song, F. Y.; Huang, Q. H.; Fan, G.  
516 R.; Wu, F. H. Chemical fingerprint and metabolic profile analysis of  
517 *Citrus reticulata* 'Chachi' decoction by HPLC-PDA-IT-MS n and  
518 HPLC-Quadrupole-Orbitrap-MS method. *J. Chromatogr. B: Anal.*  
519 *Technol. Biomed. Life Sci.* **2014**, *970*, 108–120.
- 520 (47) Fang, X. W.; Zhong, T.; Yao, G. C.; Gao, X.; Yang, M. L.; Li, H.;  
521 Le, Z. G.; Zhang, X. L. Comparison of ambient temperature and  
522 thermal surface desorption atmospheric pressure chemical ionization  
mass spectra for the pericarp of navel orange. *Chin. J. Appl. Chem.* **2015**, *32*, 1201–1207.
- (48) Chen, H. W.; Sun, Y. P.; Wortmann, A.; Gu, H. W.; Zenobi, R. *525*  
Differentiation of maturity and quality of fruit using noninvasive *526*  
extractive electrospray ionization quadrupole time-of-flight mass *527*  
spectrometry. *Anal. Chem.* **2007**, *79*, 1447–1455. *528*